

# Coherent X-Ray Generation at 2.7nm using 25fs Laser Pulses

Andy Rundquist, Zenghu Chang, Haiwen Wang, Ivan Christov,  
Henry C. Kapteyn, and Margaret M. Murnane

*Center for Ultrafast Optical Science, University of Michigan, Ann Arbor, MI 48109-2099*

*\*Permanent address: Department of Physics, Sofia University, 1126 Sofia, Bulgaria*

**Abstract.** We demonstrate for the first time that coherent soft-x-ray pulses at wavelengths of 2.7nm can be generated using 25fs driving pulses. High-order harmonic generation in He is used to produce the femtosecond x-ray harmonics, which exhibit discrete individual orders up to 221, followed by a continuum of unresolved harmonics which extend up to at least the 299th order, corresponding to a wavelength of 2.7nm, or an energy of 450eV. The large ionization potential of He, together with the ultrashort nature of the driving field, results in this dramatic extension of the harmonic plateau, by approximately 200 orders more than has been observed previously. We also obtain excellent agreement with theoretical predictions.

## INTRODUCTION

In recent years there has been much progress in developing reliable sources of coherent ultrashort light pulses in the visible and infrared regions of the spectrum.[1] At shorter wavelengths, the technique of high harmonic conversion (HHG) of an ultrashort pulse has proven most effective in generating coherent light.[2, 3] The great attraction of HHG as a source of coherent ultrafast x-ray pulses is that it is simple. A high peak-power femtosecond laser pulse is focused into an atomic gas, and the highly nonlinear interaction of the laser light with the atoms results in the emission of coherent high-order harmonics of the laser in the forward direction, as a low divergence x-ray beam. In past work, harmonic orders up to a cutoff of 135 were observed by L'Huillier et al. from the two lighter noble gases using 1ps, 1054nm laser pulses.[3] Macklin et al. observed harmonics up to a cutoff of the 109th order using 125fs, 806nm pulses in neon.[4] These previous results correspond to a minimum wavelength of  $\approx 7$ nm, or a maximum energy of  $< 170$ eV.

In this work, we present an experimental and theoretical investigation of high harmonic generation using ultrashort, 25fs, driving pulses. We find that we can dramatically extend the cutoff using shorter excitation pulses over that observed previously using longer pulses. The minimum wavelength we observe is 2.7nm, which corresponds to a harmonic order of 299, or an energy of 450eV. This work dramatically extends the available wavelength range of coherent, ultrashort-pulse, x-rays well into the "water window" region, where water is less absorbing than carbon.

## THEORETICAL

Quantum mechanical models are needed to fully describe the x-ray emission during HHG accurately.[5, 6] However, to a first approximation, quantum models can be used to describe the ionization process, while semiclassical theories can be used to describe the motion of the just-ionized electron during the first optical cycle after the ionization.[7, 8] In this picture, on the rising edge of a high intensity laser pulse, the ionization of atoms occurs via tunneling through the core potential. Once free, the electron moves in the laser field, and when the laser field reverses, the electron can return to the core with a maximum kinetic energy of  $3.17 U_p$ . Some fraction of these electrons will undergo stimulated recombination with the core, and release their energy as high harmonics. Here,  $U_p = E^2/4\omega^2$  is the ponderomotive or quiver energy (atomic units) of a free electron in an electric field  $E$  of frequency  $\omega$ . The maximum kinetic energy of  $3.17 U_p$  corresponds to an electron released at an optimum phase of the driving field - all other release phases result in lower electron energies (or even no subsequent re-encounters with the atom).

Therefore, from the above picture, the energy of the highest harmonic emitted from an atom of ionization potential  $I_p$  is predicted to be:

$$h\nu_c = I_p + 3.17 U_p \quad (1)$$

It is worth noting that  $U_p$  is evaluated at the maximum field that an electron may experience *before ionization*, even though the laser field may subsequently increase. This is because once the atoms are ionized, the x-ray emission terminates (with the possible exception of harmonic emission from ions, which is not observed here). It is also worth noting that Eqn. 1 has also been confirmed by numerical and analytic calculations, and by experimental observations for 100fs excitation laser pulsewidths or longer.

For laser pulses  $< 100$ fs, the ionization process can be strongly affected by the ultrashort rising edge of the pulse, and in the presence of finite ionization rates, the atoms survive to higher laser intensities prior to ionization.[9, 10, 11, 12] The electron is then exposed to a stronger, rapidly increasing, laser field, which allows the electron to gain even more energy prior to re-encountering the parent ion. In order to derive an explicit dependence of the cutoff photon energy ( $\nu_c$ ) on the atomic and laser parameters, we developed a simple model to predict  $\nu_c$  for given input parameters. Assuming that the atom is ionized on the leading edge of a linearly polarized laser pulse and following the method developed by Chang et al.,[13] an analytical expression of the saturation (ionization) intensity  $I_s$  can be obtained. Substituting  $U_p=9.33 \cdot 10^{14} I_s \lambda^2$  into Eqn. 1, and assuming ADK ionization rates,[14] we obtain:

$$h\nu_c = I_p + \frac{0.5 I_p^{(3+a)} \lambda^2}{\left( \ln \left( 0.86 \tau 3^{2n^*-1} G_{lm} C_{n^*,l} I_p \right) / (-\ln(1-p)) \right)^2} \quad (2)$$

where  $h\nu_c$  and  $I_p$  are in eV,  $a = 0.5$  (to correct an approximation in the derivation of the analytical expression of  $I_s$ ),  $\lambda$  is the laser wavelength in  $\mu\text{m}$ , and  $\tau$  is the FWHM of the pulse in fs. Here  $p$  is the ionization probability for defining the saturation intensity

(which is chosen to be 0.98 for our calculation),  $n^*$  is the effective principle quantum number and  $C_{n^*l^*}$  can be found in  $G_{lm}=(2l+1)(l+|m|)!/6^{|m|}l!(l-|m|)!$ , where  $l$  and  $m$  are the orbital and magnetic quantum numbers of the outermost electron. In Eqn. 2,  $C_{n^*l^*} \approx 2$ ,  $G_{lm}=3$  (except for He, where it is 1), and  $n^*$  varies between 0.74 for He and 1 for Xe. Eqn. 2 clearly shows how the cutoff photon energy changes with the laser pulse duration and wavelength, the atomic species, and the electron quantum state. These predictions are summarized in Table 1, which demonstrate that shorter duration excitation pulses should result in the generation of higher order harmonics. For comparison, the experimentally observed cutoffs for 25fs excitation pulses are also listed in Table 1, as will be discussed below. Complete quantum mechanical calculations[10, 11] show further effects for very short pulses (<25fs). For rapid risetime pulses, the phase of the atomic dipole lags that of the field, which can result in further reduced ionization due to the non-sinusoidal shape of the electric field in time.

**Table 1:** Theoretical predictions from Eqn. 2 of harmonic cutoffs for all the noble gases, for 100fs and 25fs excitation pulses (assuming the same peak intensity).

Species	Ionization Pot. (eV)	100fs cutoff order (theory)	25fs cutoff order (theory)	25fs expt.
He	24.6	239	333	299
Ne	21.6	119	163	155
Ar	15.76	45	61	61
Kr	13.99	33	41	41
Xe	12.13	23	27	29

The pulse duration of the harmonics is predicted to be short,[11] because the emission occurs only on the rising edge of the pulse. For 25fs excitation pulses, harmonics are generated during  $\approx 3$  half-cycles of the laser pulse (i.e. 3.5fs), during which time the ionization probability varies from 10% to  $\approx 100\%$ . During this time also, the amplitude of the incoming pulse changes by  $\approx 30\%$ . For very short or excitation pulses ( $\approx 5$ fs), a *single-cycle* of the excitation pulse can drive harmonic emission over a range of adjacent harmonic orders. As a result, the temporal coherence of the harmonics is dramatically improved compared with longer excitation pulses, and more efficient x-ray pulses, with durations as short as 100 attoseconds, can be emitted under the proper focusing and gas jet pressure conditions.

## EXPERIMENTAL

To observe the high harmonic cutoff energies for various gases, a setup shown in Fig. 1 was used. The Ti:sapphire laser system used for the experiments can generate TW-level, 26fs, pulses with a center wavelength of 800 nm.[15, 16] A 1cm diameter laser beam is focused onto the gas target using a 1m focal length curved mirror, which produces a  $\sim 100 \mu\text{m}$  diameter focal spot. The gas nozzle diameter is 1mm, while the gas pressure was approximately 8 torr (at the interaction region) for these experiments.

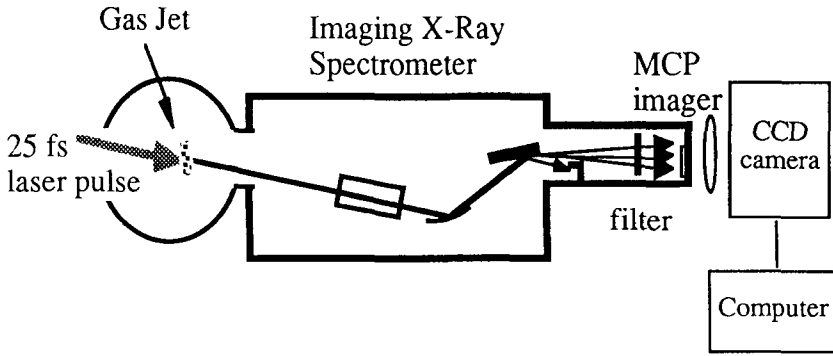


**Figure 1:** Experimental setup for high harmonic generation

Typically, 20mJ of laser energy is used to generate the harmonics, corresponding to an intensity of  $6 \times 10^{15} \text{ W/cm}^2$  at the focus. The x-rays are dispersed using a flat-field soft x-ray spectrometer, and then detected using an image intensifier with a pair of microchannel plates (MCPs). The spectrally dispersed image is recorded using a cooled CCD camera connected to a computer. It is essential to block the fundamental laser beam inside the spectrometer to prevent the generation of a significant ion background at the detector. X-ray filters must also be placed in front of the MCP to block the very bright scattered low-order harmonics.

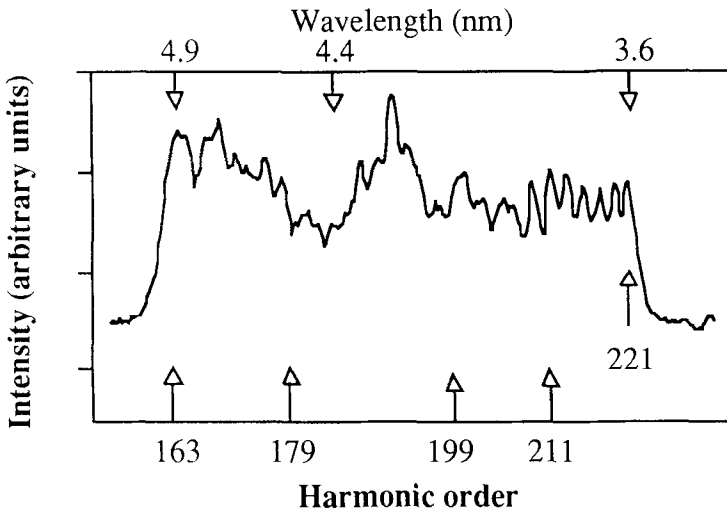


**Figure 2:** Discrete harmonic emission from helium for 25fs excitation pulses using a grating optimized for 5nm wavelengths. The cutoff at 3.6nm is instrumental.

For the experimental conditions described above, the harmonic spectra observed from Ne, Ar, Kr and Xe exhibit discrete harmonic peaks up to order 155, 61,41 and 29 respectively, as listed in Table 1. For the case of He, the harmonic spectra observed had discrete, resolvable, peaks up to the 221st order, followed by an unresolved plateau up to order  $\approx 299$ . Figure 2 shows the harmonic spectrum of He, taken using an efficient x-ray grating optimized around 50Å. The cut-off at the 221st order is instrumental, and due to a beam block placed in the spectrometer to eliminate scattered light from low-order harmonics and the fundamental light.

In order to verify experimentally that the harmonic emission is indeed due to short wavelength light, we placed a 0.4  $\mu\text{m}$  carbon filter between our spectrometer and detector. The filtered harmonic emission spectrum, on a log scale, is shown in Fig. 3(a). The position of the carbon 4.37nm absorption edge can clearly be seen, as well as the discrete harmonics, and plateau region. This also allowed us to verify our spectrometer calibration, using the position of both the carbon and boron absorption edges.

To observe shorter wavelength radiation from He, we used a grating optimized for shorter wavelengths, which allowed us to block the fundamental beam without simultaneously obscuring the harmonic radiation. However, the lower efficiency of this grating results in much lower signal-to-noise and also lower resolution. Nevertheless, we can observe harmonic radiation transmitted through a 0.2 $\mu\text{m}$  Ti filter, terminating for wavelengths shorter than the Ti edge at 2.73nm, as shown in Fig. 3(b).

From Table 1, the observed cutoff harmonic orders is in excellent agreement with theory in all cases except for He, where there is still a slight 10% difference between our experimental observation (299th) and the theoretical prediction (333rd). The good agreement between theory and experiment is most likely because our gas densities are sufficiently low and our pulses sufficiently short that propagation effects do not play a major role in determining the output. In the case of He, there are several possible explanations for the small discrepancy between theory and experiment. First, we have not definitively observed the cutoff. Second, the laser intensity in the gas medium may be well below the intensity that we used in the calculation, due to the defocusing of the laser beam induced by the ionization. Third, Eqn. 2 does not take into account propagation effects - the phase mismatch induced by the free electrons may play a significant role for efficient production of harmonics below 2.7nm. Finally, the ADK approximation and/or other assumptions made in deriving Eqn. 2 may not be valid in the case of helium, since technically ADK is valid only for large values of  $n^*$ .

Very recently, radiation at wavelengths as short as 4.4nm was observed by another group using very short driving laser pulses.[17] In this case the non transform-limited bandwidth of the driving pulses precludes the observation of discrete harmonic orders.

## SPECTRAL SHAPES

The observed harmonic spectra change dramatically with the chirp of excitation laser pulse, which can easily be varied by adjusting the separation of the stretcher gratings. As expected, the harmonic peaks shift to longer wavelengths for positive chirp, when the leading edge of the pulse is redder than the trailing edge. This result is qualitatively similar to our results with argon, but in this case the shift is larger (x2) and it can cover four harmonic orders (two peaks).

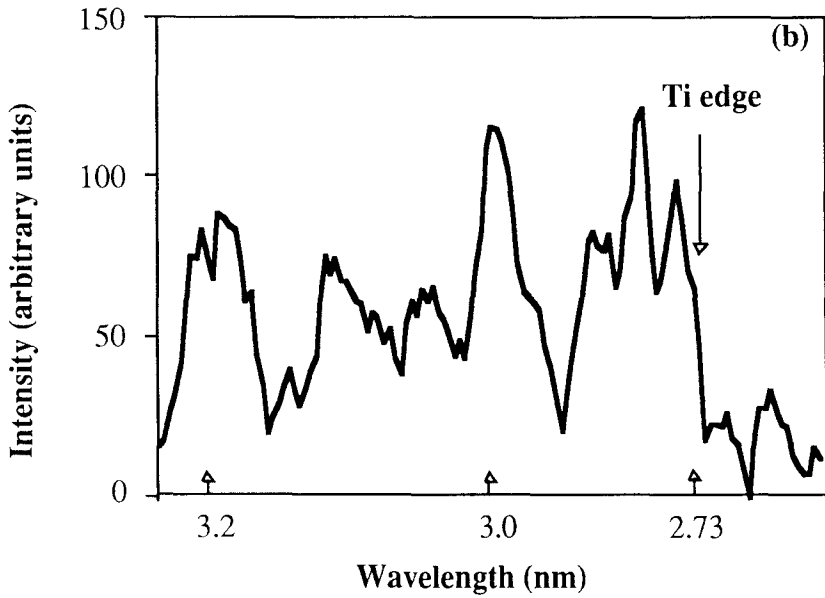
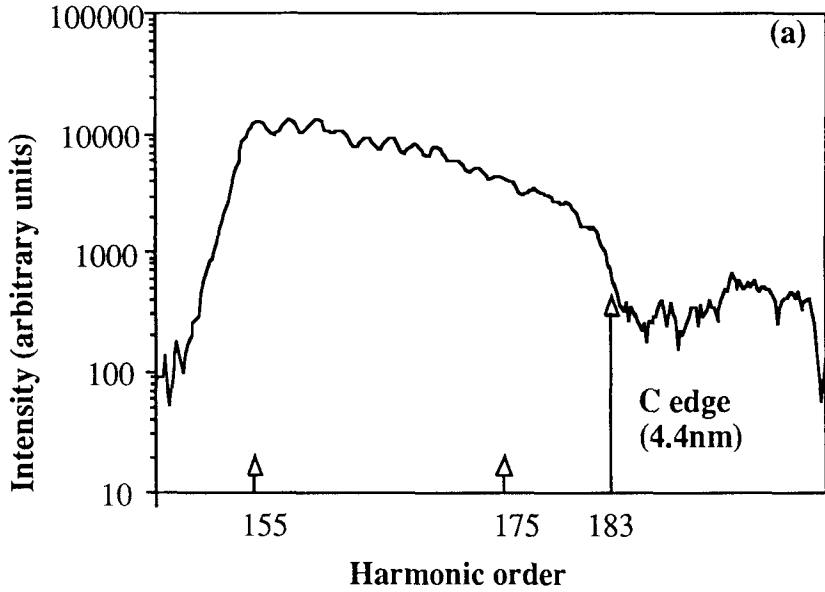


**Figure 3:** Harmonic emission from Helium, (a) filtered through a 0.4  $\mu\text{m}$  carbon filter, and (b) filtered through a 0.2  $\mu\text{m}$  titanium filter.

Finally, by increasing either the gas jet pressure or laser energy, the harmonics in the mid-plateau can merge to form a complete "x-ray continuum" source, as shown in Fig. 4. This behavior may be due to self-phase modulation and/or ionization-induced blue shifts of the excitation laser in the gas jet. It is unlikely that these effects are due to volume effects arising from different interaction and emission volumes as the laser energy is increased. The blue shift observed experimentally might arise from an increasing interaction volume if the excitation laser were positively chirped. However, we can show that the emission volume remains small since our spectrometer is imaging, which therefore spatially images in one direction, while spectrally dispersing in the perpendicular direction. It is also possible that the spectral broadening is due to some intrinsic single atom effects due to different possible trajectories of the emitting electron. However, this explanation is unlikely since the broadening disappears if the gas density is reduced. Further work is in progress to understand these effects.

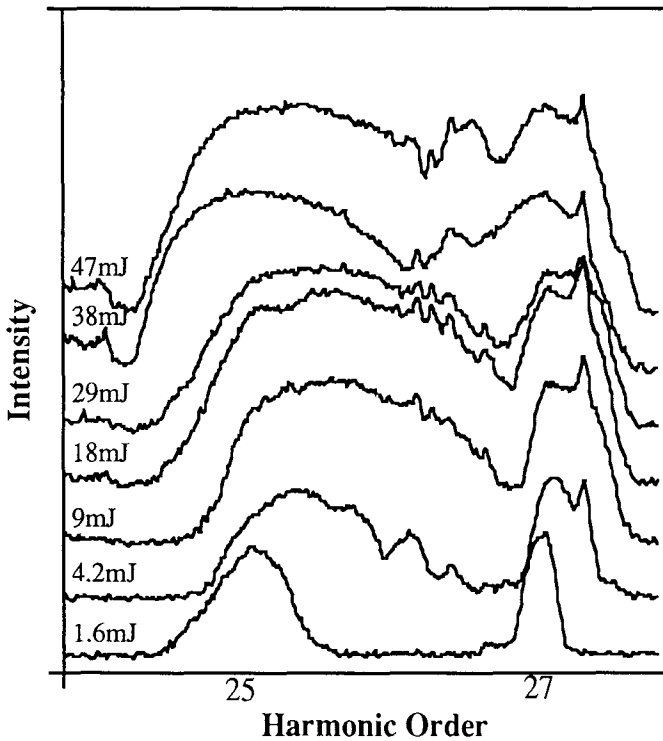


**Figure 4:** Spectral broadening and blue-shifting of the 25th harmonic in argon, as a function of incident laser energy. The cutoff on the right is due to a spectrometer aperture.

## CONCLUSION

In conclusion, we have generated coherent x-ray pulses at wavelengths of 2.7nm, which is well within the "water window" region between 4.4nm and 2.3nm, where water is less absorbing than carbon. Our shortest observed wavelength to date of 2.7nm is the shortest wavelength coherent light generated to date. These x-ray pulses are possibly a few femtoseconds in duration. Therefore, using ultrashort excitation pulses, coherent, tunable, femtosecond, x-ray beams can be generated throughout the soft-x-ray region. In the future, this very compact femtosecond x-ray source, driven by kHz repetition rate lasers, may be very important for applications such as imaging through aqueous solutions, or time-resolved photoelectron spectroscopy of organic molecules and solids.

## ACKNOWLEDGMENTS

The authors gratefully acknowledge support for this work from the National Science Foundation. We also thank Xi'an Institute of Optics and Precision Mechanics for collaboration on the microchannel plate detector used in this work. H. Kapteyn acknowledges support from an Alfred P. Sloan Foundation Fellowship.

## REFERENCES

1. A. Rundquist, C. Durfee, Z. Chang, G. Taft, E. Zeek, S. Backus, M. M. Murnane, H. C. Kapteyn, I. Christov, V. Stoev, *Applied Physics B* **65**, 161 (1997).
2. A. McPherson, G. Gibson, H. Jara, U. Johann, T. S. Luk, I. A. McIntyre, K. Boyer, C. K. Rhodes, *J. Opt. Soc. Am B* **4**, 595 (1987).
3. A. L'Huillier, P. Balcou, *Phys. Rev. Lett.* **70**, 774 (1993).
4. J. J. Macklin, J. D. Kmetec, C. L. Gordon, III, *Phys. Rev. Lett.* **70**, 766 (1993).
5. J. L. Krause, K. J. Schafer, K. C. Kulander, *Phys. Rev. Lett.* **68**, 3535 (1992).
6. K. Schafer, K. Kulander, *Physical Review Letters* **78**, 638 (1997).
7. K. C. Kulander, K. J. Schafer, J. L. Krause, in *NATO 3rd Conference on Super Intense Laser-Atom Physics* Han-sur-Lesse, Belgium, 1993).
8. M. Lewenstein, P. Balcou, M. Y. Ivanov, P. B. Corkum, *Physical Review A* **49**, 2117 (1993).
9. J. Zhou, J. Peatross, M. M. Murnane, H. C. Kapteyn, I. P. Christov, *Physical Review Letters* **76**, 752 (1996).
10. I. P. Christov, J. P. Zhou, J. Peatross, A. Rundquist, M. M. Murnane, H. C. Kapteyn, *Physical Review Letters* **77**, 1743 (1996).
11. I. P. Christov, M. M. Murnane, H. C. Kapteyn, *Physical Review Letters* **78**, 1251 (1997).
12. Z. Chang, A. Rundquist, H. Wang, H. C. Kapteyn, M. M. Murnane, to be published in *Physical Review Letters* (1997).
13. B. Chang, P. Bolton, D. Fittinghoff, *Phys. Rev. A* **47**, 4193 (1993).
14. M. Ammosov, N. Delone, *Sov. Phys. JETP* **64**, 1191 (1986).
15. J. Zhou, C. P. Huang, C. Shi, M. M. Murnane, H. C. Kapteyn, *Opt. Lett.* **19**, 126 (1994).
16. J. Zhou, C. P. Huang, M. M. Murnane, H. C. Kapteyn, *Optics Letters* **20**, 64 (1994).
17. C. Spielmann et al., in *Quantum Electronics and Laser Science Conference, Paper QPD 4* (OSA, Baltimore, MD, 1997)